P1 1174997

THE UNITED STATES OF AMERICA

TO ALL TO WHOM THESE PRESENTS SHALL COME:

UNITED STATES DEPARTMENT OF COMMERCE
United States Patent and Trademark Office

May 25, 2004

THIS IS TO CERTIFY THAT ANNEXED HERETO IS A TRUE COPY FROM THE RECORDS OF THE UNITED STATES PATENT AND TRADEMARK OFFICE OF THOSE PAPERS OF THE BELOW IDENTIFIED PATENT APPLICATION THAT MET THE REQUIREMENTS TO BE GRANTED A FILING DATE.

APPLICATION NUMBER: *60/461,212*
FILING DATE: *April 07, 2003*
RELATED PCT APPLICATION NUMBER: *PCT/US04/10882*

By Authority of the
COMMISSIONER OF PATENTS AND TRADEMARKS

H. L. Jackson

H. L. JACKSON
Certifying Officer

PRIORITY DOCUMENT
SUBMITTED OR TRANSMITTED IN COMPLIANCE WITH RULE 17.1(a) OR (b)

04-09-03. 60461212.04P70

A/Pto

PTO/SB/16 (10-01)
Approved for use through10/31/2002. OMB 0651-0032
U.S. Patent and Trademark Office; U.S. DEPARTMENT OF COMMERCE

Under the Paperwork Reduction Act of 1995, no persons are required to respond to a collection of information unless it displays a valid OMB control number.

PROVISIONAL APPLICATION FOR PATENT COVER SHEET

This is a request for filing a PROVISIONAL APPLICATION FOR PATENT under 37 CFR 1.53(c).

Express Mail Label No. EU654844426US

INVENTOR(S)

Given Name (first and middle [if any])	Family Name or Surname	Residence (City and either State or Foreign Country)
Michael J.	Antal, Jr.	Honolulu, Hawaii

☐ Additional inventors are being named on the _____ separately numbered sheets attached hereto

TITLE OF THE INVENTION (500 characters max)

Biocarbon Fuel Cell Electrode

CORRESPONDENCE ADDRESS

Direct all correspondence to:

☐ Customer Number _____ → Place Customer Number Bar Code Label here

OR Type Customer Number here

☒ Firm or Individual Name	University of Hawaii				
Address	2800 Woodlawn Drive, Suite 280				
Address					
City	Honolulu	State	Hawaii	ZIP	96822
Country	USA	Telephone	(808) 539-3817	Fax	(808) 539-3833

ENCLOSED APPLICATION PARTS (check all that apply)

☒ Specification Number of Pages 45

☐ Drawing(s) Number of Sheets

☐ Application Data Sheet. See 37 CFR 1.76

☐ CD(s), Number

☐ Other (specify)

METHOD OF PAYMENT OF FILING FEES FOR THIS PROVISIONAL APPLICATION FOR PATENT

☒ Applicant claims small entity status. See 37 CFR 1.27.

☒ A check or money order is enclosed to cover the filing fees

☐ The Commissioner is hereby authorized to charge filing fees or credit any overpayment to Deposit Account Number: _____

☐ Payment by credit card. Form PTO-2038 is attached.

FILING FEE AMOUNT ($): $80.00

The invention was made by an agency of the United States Government or under a contract with an agency of the United States Government.

☒ No.

☐ Yes, the name of the U.S. Government agency and the Government contract number are: _____

Respectfully submitted,

SIGNATURE Richard F. Cox

Date 4/7/2003

TYPED or PRINTED NAME Richard F. Cox, Jr.

REGISTRATION NO. (if appropriate)

TELEPHONE (808) 539-3817

Docket Number: 00245

USE ONLY FOR FILING A PROVISIONAL APPLICATION FOR PATENT

This collection of information is required by 37 CFR 1.51. The information is used by the public to file (and by the PTO to process) a provisional application. Confidentiality is governed by 35 U.S.C. 122 and 37 CFR 1.14. This collection is estimated to take 8 hours to complete, including gathering, preparing, and submitting the complete provisional application to the PTO. Time will vary depending upon the individual case. Any comments on the amount of time you require to complete this form and/or suggestions for reducing this burden, should be sent to the Chief Information Officer, U.S. Patent and Trademark Office, U.S. Department of Commerce, Washington, D.C. 20231. DO NOT SEND FEES OR COMPLETED FORMS TO THIS ADDRESS. SEND TO: Box Provisional Application, Assistant Commissioner for Patents, Washington, D.C. 20231.

FEE TRANSMITTAL for FY 2003

Effective 01/01/2003. Patent fees are subject to annual revision.

☑ Applicant claims small entity status. See 37 CFR 1.27

TOTAL AMOUNT OF PAYMENT ($) 80.00

Complete if Known	
Application Number	
Filing Date	04/7/2003
First Named Inventor	Michael J. Antal, Jr.
Examiner Name	
Art Unit	
Attorney Docket No.	TLG-00245

METHOD OF PAYMENT *(check all that apply)*

☑ Check ☐ Credit card ☐ Money Order ☐ Other ☐ None

☐ Deposit Account:

Deposit Account Number

Deposit Account Name

The Commissioner is authorized to: *(check all that apply)*

☐ Charge fee(s) indicated below ☐ Credit any overpayments

☐ Charge any additional fee(s) during the pendency of this application

☐ Charge fee(s) indicated below, **except for the filing fee** to the above-identified deposit account.

FEE CALCULATION

1. BASIC FILING FEE

Large Entity Fee Code	Large Entity Fee ($)	Small Entity Fee Code	Small Entity Fee ($)	Fee Description	Fee Paid
1001	750	2001	375	Utility filing fee	
1002	330	2002	165	Design filing fee	
1003	520	2003	260	Plant filing fee	
1004	750	2004	375	Reissue filing fee	
1005	160	2005	80	Provisional filing fee	80.00

SUBTOTAL (1) ($) 80.00

2. EXTRA CLAIM FEES FOR UTILITY AND REISSUE

	Extra Claims		Fee from below		Fee Paid
Total Claims		-20** =		X	=
Independent Claims		- 3** =		X	=
Multiple Dependent					=

Large Entity Fee Code	Large Entity Fee ($)	Small Entity Fee Code	Small Entity Fee ($)	Fee Description
1202	18	2202	9	Claims in excess of 20
1201	84	2201	42	Independent claims in excess of 3
1203	280	2203	140	Multiple dependent claim, if not paid
1204	84	2204	42	** Reissue independent claims over original patent
1205	18	2205	9	** Reissue claims in excess of 20 and over original patent

SUBTOTAL (2) ($)

***or number previously paid, if greater; For Reissues, see above*

FEE CALCULATION (continued)

3. ADDITIONAL FEES

Large Entity Fee Code	Large Entity Fee ($)	Small Entity Fee Code	Small Entity Fee ($)	Fee Description	Fee Paid
1051	130	2051	65	Surcharge - late filing fee or oath	
1052	50	2052	25	Surcharge - late provisional filing fee or cover sheet	
1053	130	1053	130	Non-English specification	
1812	2,520	1812	2,520	For filing a request for *ex parte* reexamination	
1804	920*	1804	920*	Requesting publication of SIR prior to Examiner action	
1805	1,840*	1805	1,840*	Requesting publication of SIR after Examiner action	
1251	110	2251	55	Extension for reply within first month	
1252	410	2252	205	Extension for reply within second month	
1253	930	2253	465	Extension for reply within third month	
1254	1,450	2254	725	Extension for reply within fourth month	
1255	1,970	2255	985	Extension for reply within fifth month	
1401	320	2401	160	Notice of Appeal	
1402	320	2402	160	Filing a brief in support of an appeal	
1403	280	2403	140	Request for oral hearing	
1451	1,510	1451	1,510	Petition to institute a public use proceeding	
1452	110	2452	55	Petition to revive - unavoidable	
1453	1,300	2453	650	Petition to revive - unintentional	
1501	1,300	2501	650	Utility issue fee (or reissue)	
1502	470	2502	235	Design issue fee	
1503	630	2503	315	Plant issue fee	
1460	130	1460	130	Petitions to the Commissioner	
1807	50	1807	50	Processing fee under 37 CFR 1.17(q)	
1806	180	1806	180	Submission of Information Disclosure Stmt	
8021	40	8021	40	Recording each patent assignment per property (times number of properties)	
1809	750	2809	375	Filing a submission after final rejection (37 CFR 1.129(a))	
1810	750	2810	375	For each additional invention to be examined (37 CFR 1.129(b))	
1801	750	2801	375	Request for Continued Examination (RCE)	
1802	900	1802	900	Request for expedited examination of a design application	

Other fee (specify) _____

*Reduced by Basic Filing Fee Paid

SUBTOTAL (3) ($)

SUBMITTED BY

Name (Print/Type)	Richard F. Cox, Jr.	Registration No. (Attorney/Agent)	(Complete *if applicable*)
Signature			Telephone 808-539-3817
			Date 04/7/2003

WARNING: Information on this form may become public. Credit card information should not be included on this form. Provide credit card information and authorization on PTO-2038.

If you need assistance in completing the form, call 1-800-PTO-9199 (1-800-786-9199) and select option 2.

3/28/2003

Electrical and Physical Properties of Carbonized Charcoals

Kazuhiro Mochidzuki, Florence Soutric, Katsuaki Tadokoro, Michael Jerry Antal, Jr.*

Hawaii Natural Energy Institute, University of Hawaii at Manoa, Honolulu, Hawaii 96822

Mária Tóth

Hungarian Academy of Sciences, Research Center for Earth Sciences, Laboratory for Geochemical Research, Budaörsi út 45, Budapest, Hungary 1112.

Borbála Zelei and Gábor Várhegyi

Hungarian Academy of Science, Chemical Research Center, Research Laboratory of Materials and Environmental Chemistry, P. O. Box 17, Budapest 1525, Hungary

Abstract

Because coal does not conduct electricity and graphite is costly and inert, little attention has been given to the development of a fuel cell that utilizes a consumable carbon anode to generate power. In this work we show that a packed bed of carbonized charcoal particles subject to a compressive pressure (ca. 8 MPa) can be a good electrical conductor ($\sigma < 0.2$ Ω-cm). Low electrical resistivities σ are manifest by many different charcoals after carbonization at a heat treatment temperature (HTT) of 950 °C. Although the resistivity of a packed bed of a specific carbonized charcoal decreases as a weak function of increasing apparent density of the bed, low density carbonized charcoal beds (e.g. Leucaena wood) can manifest higher electrical conductivities than high density packed beds (e.g. macadamia nut shell). The 7 order of magnitude decrease in the electrical resistivity of charcoal with increasing HTT is not associated with any dramatic change in the carbons' x-ray diffraction spectrum, its FTIR spectrum, or its elemental analysis. Since charcoal powder is competitive in price with fossil fuels, and since carbonized charcoal is extremely reactive, it appears that a packed bed of carbonized charcoal

charcoal is extremely reactive, it appears that a packed bed of carbonized charcoal hold promise as a consumable anode for use in a fuel cell. {More?? }

Introduction

Carbon batteries played an important role in the history of fuel cell research. Sixteen years after Grove[1] demonstrated an "electrolyte gas cell" that gave an open circuit EMF of about 1 V between H_2 and O_2, Becquerel attempted to build a fuel cell that consumed coal.[2, 3] Unfortunately, the electrolyte contained a nitrate that attacked the carbon without producing a current. Later Jablockoff[2, 3] tested an apparatus modeled on a similar concept. By the end of the 19th century the increasing production of electric power began to consume considerable amounts of coal because the conversion efficiency was low (3%).[1] Contemplating this problem, in 1894 Ostwald[1] called for development of a fuel cell that would react carbon with oxygen to produce electricity more efficiently than therrmo-mechanical equipment. Two years later in Boston Jacques[1] demonstrated a 1.5 kW battery that employed a consumable carbon anode, an iron cathode, and an air-bubbled alkali hydroxide electrolyte to generate 0.9 V at 400 – 500 °C. Operating intermittently, this battery delivered power with an overall efficiency of 32% during a six-month period. The experiment failed because carbonates accumulated in the electrolyte that halted the electrochemistry.[1] In 1904 Haber and Bruner[1] showed that the Jacques carbon fuel cell actually involved the production of hydrogen as an intermediate in the electrochemistry. But Haber was unable to build a practical carbon fuel cell. In 1937 Baur and Preis[3] tested a fuel cell that used a coke anode and an electrolyte composed of zirconia stabilized with magnesia or yttria at >1000 °C. Vielstich explains that the high temperature was needed because of the low reactivity of the carbon fuel.[1] No practical carbon fuel cells resulted from the work of Baur and Preis.

Interest in carbon fuel cells resurfaced during the 1970's, when the Stanford Research Institute (SRI) attempted to develop a coal based fuel cell that employed molten lead at temperatures of 500 to 900 °C.[4,5] This work was abandoned in 1981. Recently, Scientific Applications and Research Associates[6] reported progress in further developing the SRI concept. At Stanford University Gur and Huggins[7] demonstrated a high temperature (725 to 955 °C) fuel cell that employed stabilized zirconia as a solid electrolyte and a graphite anode. To the best of our knowledge, these recent developments have not led to the demonstration of a practical carbon fuel cell. Summarizing the status of carbon fuel cells, Bockris and Srinivasen[3] concluded that carbon fuel cells are impractical because (i) coal is not an electrical conductor, and (ii) graphite is too scarce and expensive to be used as a fuel. Thus the history of carbon fuel cell research suggests that the chief obstacles to the development of a biocarbon fuel cell are the electrical conductivity of the biocarbon, its cost, and its reactivity.

It has been known for centuries that biocarbons can possess very high electrical conductivities. In 1810 carbonized charcoal electrodes were used in an arc lamp, and in 1830 carbonized charcoal was used as an electrode for primary batteries. These electrodes were made from powdered charcoal or coke bonded with sugar syrup or coal tar, pressed and carbonized.[8] Recently, Coutinho, Luengo, and their co-workers[9-11] reported extensive studies of biocarbon electrodes manufactured from charcoal particles bonded together by wood tar and subsequently carbonized. At a carbonization temperature of 900 °C biocarbons from Eucalyptus wood began to evidence a turbostratic (i.e. microcrystalline) structure as revealed by XRD.[9,11] The measured electrical resistivity of the electrode fell to 10^{-2} Ω–cm for carbonization at temperatures above 900 °C. This background suggests that carbonized charcoal could be used to fabricate the consumable anode of a carbon battery. Furthermore, we remark that charcoal can be produced from biomass inex-

pensively in yields that approach the theoretical limit.[12, 13] Carbonized charcoal is also easy to store, and an established infrastructure exists to deliver charcoal to consumers worldwide. Moreover, carbonized charcoal - unlike graphite - is extremely reactive.[14-17] For these reasons we have a keen interest the development of biocarbon fuel cells. The first step is to establish some baseline data for the properties of carbonized charcoal electrodes. In this paper we present data that describe the effects of increasing carbonization temperature on the properties of carbonized charcoal particles, including their electrical resistivity in a packed bed subject to compressive force, their chemical and physical composition as determined by elemental analysis, FTIR, and XRD spectra, and their surface area. We focus on a carbonization temperature of 950 C because earlier work has proven the high reactivity of this biocarbon.[14-17] Higher carbonization temperatures may produce reactive carbons with even lower electrical resistivities than those described in this report.

Apparatus and experimental procedures

The raw biomass materials that served as substrates to produce the high-yield charcoals employed in this study were obtained as representative grab-samples in Hawaii. The high-yield charcoals were produced according to procedures described in earlier publications.[12]

Carbonization procedures. A tubular furnace (Applied Test Systems 3210) with temperature control (Applied Test Systems XT-16), which can reach temperatures as high as 1200 °C, was employed to carbonize the high-yield charcoal samples. A quartz tube (122 cm long, 1.99 cm I.D.) was placed within the furnace and used to carbonize a measured amount of charcoal in a ceramic boat. By locating type K thermocouples in the boat, it was possible to accurately measure the heat treatment temperature (HTT) of the charcoal. UHP nitrogen gas was delivered at 1.0

L/min to the tube during the carbonization process, thereby ensuring that the carbonization process, including the heat-up and cool-down steps, occurred in an inert environment. In a few cases, charcoals were carbonized within a closed crucible in a muffle furnace (Barnstead Themolyne FB1215M). This procedure was employed in our earlier work,[12] and is able to carbonize larger quantities of charcoal more conveniently than the tubular furnace. Unfortunately, several weaknesses accompany the use of a muffle furnace. First (and perhaps foremost), the muffle furnace thermocouple (TC) reports its own temperature, which is neither the temperature of the furnace nor the temperature of the carbon within the closed crucible. Our studies indicate that the muffle furnace TC reports a temperature about 30 to 40 °C higher than the temperature of the outer surface of the ceramic crucible. The measurement of the carbon temperature within the closed crucible is not easy; consequently, we do not know how large a temperature gradient exists between the outer surface of the crucible and the center of the carbon bed in the closed crucible. Secondly, the lid of the crucible leaks a little air; consequently, the carbonization is not accomplished in a truly inert environment.

FTIR analyses. The FTIR spectra were measured by a FTIR spectrometer system (Perkin-Elmer 1710), including a DTGS detector, DRIFT accessory and microsampling. The specimens were measured in powder form, using KBr as reference material. The spectra were recorded from 4400 to 400 cm^{-1} by averaging 100 scans at 4 cm^{-1} resolution.

XRD analyses. X-ray powder diffraction (XRD) measurements were carried out for phase and crystal structure identification with Philips PW1710 diffractometer using CuK_a radiation and a graphite monochromator (45 kV, 35 mA, divergence 1°). {GV & MT: OK?? More??}

BET surface area and total pore volume analyses. An automatic gas analyzer (Quantachrome Aurosorb-1) was used to determine the specific surface area and total pore volume of the

carbonized charcoals. After a vacuum outgas step at 483 K for 4 hours, the nitrogen-adsorption isotherm was measured at a liquid-nitrogen temperature (77 K). The Brunauer-Emmett-Teller (BET) method was employed to determine the surface area from a limited linear region of the adsorption isotherm, usually $0.05 < P/P_0 < 0.35$. The total pore volume was calculated from the amount of nitrogen adsorbed at a relative pressure close to unity ($P/P_0 > 0.99$). To validate our surface area determinations, we measured the surface area of a commercial Barnebey and Sutcliffe (B&S) coconut shell activated carbon. Our result (1201 m^2/g) agreed with the value reported by B&S (1106 m^2/g).

Electrical resistivity. The electrical resistivity of the biocarbon samples was determined by a two-probe packed-bed technique at room temperature (*ca.* 20 °C). As shown in Figure 1, the Nickel electrodes at the top and bottom of the 1.9 cm packed bed - contained in an alumina tube - enable measurement of the electrical resistance of the bed. The packed bed is compressed by the upper electrode, which is forced against the bed by a pneumatic piston. Note that the electrodes are insulated from the apparatus by Teflon and almina. The electrical resistance of the packed bed is measured with a precision ISOTEK M210 4 probe?? {MJA??} ohmmeter. This meter has a resolution of 0.001Ω from 0 to 1.990Ω, a resolution of 0.01Ω from 1.99Ω to 19.90Ω, and a resolution of 0.1Ω from 19.9Ω to 199.9Ω. Our setup mimics the apparatus originally employed by Mrozowski[18] in his pioneering work, but was designed to enable its future use as the anode of a carbon fuel cell within a pressure vessel. The resistivity, ρ in Ω·cm, is given by the equation, $\rho = RA/l$, where R, A and l are measured resistance in Ω, cross sectional area of the bed in cm^2 and length between the probes in cm, respectively. Note that the measured length is not the exact length l of the bed due to the compression of the nickel electrode and the stretching of the stainless steel threaded rods that results from the compressive force applied to the packed bed.

To account for these effects we measured the change in the apparent length of an empty bed (i.e. zero length offset) over the range of applied pressures used in this work (see Figure2). After an initial small, nonlinear change in length (due to slack in the system) the change in the zero offset length was linear with pressure. The Hook's law slope of the line (-3.23??{KT: OK??} $\times 10^{-3}$ cm/MPa) displayed in Figure 2 is nearly identical to the theoretical value (-3.34??{KT:.OK?? $\times$ 10^{-3} cm/MPa) calculated using the appropriate Young's moduli of Ni 200 and SUS 316 and geometric factors for the elements of the cell under compression and tension. We used the Hook's law formula to correct the zero offset value of the instrument, and this correction resulted in a small decrease in the calculated values of the packed bed's resistivity and its density. Higher compressive pressures and the shorter bed lengths had a bigger impact on this correction. In the case of a compressive pressure of 9.5MPa and a bed length of 0.1 cm, the correction resulted in *ca.* 35% decrease of the measured resistivity and the apparent density of the packed bed.

Results

Unless noted otherwise, the carbons listed in Table 1 were prepared in the tubular furnace at the indicated HTT with a soak time of 10 min. Typically two to three boat lots were needed to produce enough carbonized charcoal for subsequent analyses. As expected, the burnoff of the macshell charcoal increased monotonically with increasing HTT, except for the 1050 °C sample that was derived from a different charcoal batch with a much lower volatile matter content. The elemental analyses of these carbons showed a scattered progression from 87.9 wt% to 95.13 wt% carbon with increasing HTT accompanied by concomitant decreases in the H and O content of samples. Note that the 1050 °C carbon was derived from a different macshell charcoal sample than the other carbons and this might explain its high nitrogen content. Values of the H/C and

O/C ratios of the macshell carbons (see Table 2) decreased monotonically, except for the 950 °C sample. Of the remaining carbons listed in Tables 1 and 2, the leucaena wood carbon resembles the kukui nut shell carbon (except for their respective ash contents). A comparison of the 950 °C carbons reveals a considerable range in the values of each of the properties listed in Tables 1 and 2.

FTIR Analyses. The FTIR spectra of the macshell carbons prepared at 650 to 850 °C are displayed in Figure 3. For comparison, the spectrum of the macshell charcoal substrate and that of a Sigma-Aldrich synthetic graphite are also indicated. Note that all spectra are displayed on a linear absorbance scale and each curve is drawn one unit higher than the one beneath it. This approach facilitates the comparison of the relative intensity of the spectra. Weak features at about 2350 cm^{-1} belong to CO_2 absorption of air. H_2O adsorbed on the KBr reference material gives weak, broad inverse bands at about 3400 and 1630 cm^{-1} in the spectra of the carbons. There is a weak and sharp absorption band at about 1378 cm^{-1} originating from a KBr impurity.

As expected, the macshell charcoal has an alkyl aromatic structure with many oxygen containing (C-O-H, C=O, C-O-C) functional groups that give rise to characteristic bands in the infrared spectrum.[19] During carbonization these functional groups are destroyed. At 650 °C the O-H groups (3700-2000 cm^{-1}), the aliphatic C-H groups (3000-2800 cm^{-1}) and in a great part the C=O groups (~1700 cm^{-1}) decompose, and condensed aromatic structures form with characteristic C-H out-of-plane bending modes (three main band components) between 900 and 700 cm^{-1}. These findings corroborate earlier TG-MS studies of the carbonization of macshell charcoal.[19, 20] The TG-MS data revealed major peaks associated with the evolution of H_2O, CH_4, CO, and CO_2 below 650 °C. At 750 °C most of the aromatic C-H groups are lost. This loss corresponds to a TG-MS peak in the evolution of H_2 at about 750 °C. A weak C-H absorption remains at about

880 cm^{-1}. It is assigned to lone H-atoms at the edges of the condensed aromatic sheets.[21] A weak, broad band with some sub-bands can be observed between 1700 and 1000 cm^{-1} due to the skeletal stretching and bending modes of aromatic structures containing residual O and/or N hetero atoms. At 850 °C the intensity of this weak, broad feature further diminishes, and so does the aromatic C-H (~880 cm^{-1}) band, as well.

With increasing carbonization temperature between 650 and 850 °C the overall intensity of the infrared spectrum decreases along with the loss of functional groups. The baseline in the spectra of the carbonized charcoals is shifted upward. This baseline shift (increasing diffuse absorption) is assigned to low energy electron excitations of condensed aromatic structures. It is a well-known phenomenon in carbonized coal spectra.[21] Graphite has no characteristic infrared band(s) in the investigated spectral region and the FTIR method is not sensitive to long-range ordering during graphitization.[22] Graphitization can be followed by Raman spectroscopy;[23] however, the best method is XRD[24] (see below).

All the carbons obtained from the macadamia nut shell, leucaena, coconut husk and kukui nut shell charcoals with HTT of 950 °C show very similar spectra to each other, as well as to the spectrum of graphite (see Figure 4). Leucaena has the highest N content, but the spectra of carbons obtained from this precursor do not show significant differences in the region of the C=N and C-N stretching bands between 1700 and 1000 cm^{-1} from the spectra of other carbons. Small differences in the baseline positions and shapes can probably be accounted for particle size and scattering effects rather than electron mobility changes. These effects hardly can be eliminated from the DRIFT spectra of the carbonized charcoals and graphite.

XRD Analyses. For reference, Figure 5 displays XRD spectra of synthetic and natural graphite samples. Figure 6 displays spectra of macadamia shell charcoals carbonized at increasing

temperatures. Unexpectedly, the XRD spectra undergo almost no visible change with increasing HTT above 750 °C. Table 3 demonstrates this observation. The scattering domain contains only 2 layers in the 002 direction. The estimated aromaticity γ_a [25, 26] of these domains does not significantly increase with HTT above 750 °C. {GV & MT: what is ε?? What can we say about it??} Figure 7 displays the XRD spectra of the 950 °C carbonized charcoals. These spectra are similar, except for the presence of small peaks that arise from the presence of inorganic species (mineral impurities) in the carbon. The broad, featureless peaks displayed in Figure 7 bear little resemblance to the broad peak at $2\theta = 25°$ associated with the XRD spectra of a turbostratic carbon (Monarch 71) displayed in Figure 5 of Walker and Seeley,[27] the heat-treated coals and petroleum coke displayed in Figure 4 of Senneca et al.[28], or the sharp peaks associated with heat-treated Australian black coals reported by Lu et al.[25] As indicated in Table 3, the scattering domain of these carbons contains less than 2 layers in the 002 direction. Values of ε for these carbons exceed that of the 750 °C macnut shell carbon. The aromaticity of these carbons is high, but significantly lower than that of graphite.

Surface Area and Pore Volume Distributions. Table 1 displays the BET surface areas and (in some cases) the total pore volumes of the carbonized charcoal samples discussed above. Although the carbonization technique employed in this study was not designed to enhance the porous structure of the substrate, some of the biocarbon samples evidenced surprisingly high BET surface areas (e.g. 437 m^2/g). Earlier workers reported values between 100 and 200 m^2/g for macshell charcoal carbonized at 900 to 950 C.[14-17, 29] In the case of the macshell carbon, the lack of a clear trend in the development of surface area with increasing HTT may reflect gross heterogeneities in the surface properties of the macshell charcoal. Both Macadamia nut and Kukui nut shells are rich in oil that forms a coke during pyrolysis. This coke must have a low sur-

face area. It is possible that the scatter in the macshell data, and the very low surface area of the Kukui shell carbon are a result of coked nut oils. More generally, we remark that 50 years ago Rosalind Franklin called attention to the existence of "a large volume of extremely small holes" within highly porous, non-graphitizing carbons (e.g. sugar charcoal).[30] The presence of extremely narrow pores in the biocarbons listed in Table 1 complicates the determination of their surface areas and pore volume distributions.

Electrical resistivity. Because few studies have been reported of the electrical properties of packed beds of biocarbons, we initiated this work with measurements of a commercially available B&S coconut shell activated carbon (AC), and a commercial graphite powder that serve as reference materials. The B&S AC is attractive because it can be sieved to a useful particle size (20/40 mesh) and it is quite homogeneous. The graphite powder is a logical reference material, but its very fine particle size makes it difficult to handle.

Figure 8a displays the resistivity and bed length as a function of applied compressive pressure for a 0.506 g packed bed of 20/40 mesh AC. After an initial compression of the bed, the influence of the compressive pressure on the measured resistivity and length of the bed, and its apparent density is reproducible with little hysteresis. Although Mrozowski[18] observed creep in his measurements of packed bed resistivity, we detected no significant, systematic creep over a 60 min period. The creep observed by Mrozowski may have resulted from the very high compressive pressures used in his work. In Figure 8a the resistivity of the bed decreases to a value of 0.41 Ω-cm at a density of 0.61 g/mL under a compressive pressure of 7.63 MPa. Note that after the initial compaction, the packed bed is virtually incompressible. Figures 8b and 8c display identical behavior for packed beds of 1.0 g and 1.5 g (respectively). Figure 8d confirms the expected ohmic behavior of the packed bed under a compressive pressure of 7.6 MPa. The slope of

the least-squares line yields a resistivity of 0.44 Ω-cm. This value is in good agreement with the individual single point values. Note that the contact resistance, given by the y intercept of the line, is negligible at this pressure. Concerning the contact resistance, Marchand[31] comments: "A significant value of the electrical conductivity, that is a value, which is indicative of the actual structure of the aromatic or graphitic units, can only be obtained if the parasitic contact resistances between particles are reduced to a negligible minimum. This obviously could be achieved by applying a sufficient external pressure to the sample." Related data for a smaller particle size (< 105 μm) are displayed in Figure 8e. In this case the AC reaches a density of 0.81 g/mL (see Table 4) with a resistivity of 0.26 Ω-cm under a compressive pressure of 11.5 MPa. At 7.86 MPa the measured resistivity (0.35 Ω-cm) of the < 105 μm powder (with a bed density of 0.78 g/mL) is somewhat less than the value (0.41 Ω-cm) associated with the 20/40 mesh material (with a bed density of 0.61 g/mL) under a compressive pressure of 7.63 MPa. This comparison suggests that the electrical resistivity of the packed bed is not strongly dependent upon either the particle size or the apparent density of the bed (see below).

Figure 9 displays similar data for a 2.00 g packed bed of 1-2 μm graphite powder. The very fine particle size combined with the lubricity of graphite powder causes the bed to be unusually compressible. Under a compressive pressure of 7.77 MPa it evidenced a resistivity of 0.029 Ω-cm at a density of 1.41 g/mL. We remark that the compressive pressure caused the packed bed of graphite particles to become a wafer that retained its integrity when removed from the apparatus, although the wafer was easily broken by hand. By way of comparison, the density of solid graphite is 2.23 g/mL, and the electrical resistivity of single crystals of graphite is anisotropic, with values as low as 40 μΩ–cm in the a-b plane at 300 K.[32]

We have no knowledge of the conditions that were employed by Barnebey and Sutcliffe to produce the AC used to acquire the data displayed in Figure 8. In particular, we have no knowledge of the carbon's heat treatment temperature (HTT), i.e. its peak temperature. To put a floor on this value we carbonized the AC according to our usual procedure in the muffle furnace at 950 °C and measured its resistivity as a function of compressive pressure. The values displayed in Figure 10 follow trends similar to those of Figure 8 but with a resistivity of 0.25 Ω·cm and a density of 0.60 g/mL under a compressive pressure of 7.61 MPa. The carbonization treatment had little effect on the packed bed density, but it lowered the resistivity by 43%. Evidently, the activation treatment employed by Barneby and Sutcliffe did not involve a peak temperature above 950 °C. Data for carbonized coconut husk charcoal powder displayed in Figure 11 can be compared to that displayed in Figure 10. Under a compressive pressure of 7.77 MPa the carbonized husk charcoal offers a resistivity of 0.19 Ω·cm at a density of only 0.45 g/mL. In spite of its low density, the coconut husk carbonized charcoal is a better conductor of electricity than the commercial coconut shell AC. Ostensibly this result appears to contradict the claim of some earlier workers [33,34,35] that increasing the porosity of a carbon decreases both its thermal and its electrical conductivities. We remark that oxygen chemisorption can increase the electrical resistivity of a carbon,[36] hence the relatively low conductivity of the activated carbon may reflect its aggressive chemisorption of oxygen from the air.

As shown in Figure 12a a packed bed of the 20/40 mesh macshell carbonized charcoal (950 °C) evidences an electrical resistivity of 0.12 Ω-cm at a density of 0.53 g/mL under a compressive pressure of 7.97 MPa. In order to learn more about the effects of HTT on the electrical resistivity of carbonized charcoals, we also carbonized macshell charcoal at HTT of 1050, 850, 750, and 650 °C. Figure 12b displays the effect of increasing compressive pressure on the resis-

tivity of each of these carbons, that decreases by more than seven orders of magnitude with increasing HTT from 650 to 1050 °C. As displayed in Figure 12b, the 1050 C macshell carbon's resistivity is about twice that of the graphite powder. Because these values approach the limit of detectability of our equipment, the exact ratio may differ somewhat from a factor of two. Under a compressive pressure of 7.8 MPa the apparent density of the packed bed decreases from 0.71 to 0.58 g/mL as the HTT increases from 650 to 950 °C. This decrease is due to increased porosity of the carbon at higher HTT.

The 20/40 mesh Kukui shell carbon (see Figure 13) evidences a similar electrical resistivity (0.18 Ω-cm) to those of the coconut husk and macshell carbons, but at a density of 0.82 g/mL. The apparent density (0.44 g/mL) of the 20/40 mesh Leucaena wood carbonized charcoal at 7.61 MPa (see Figure 14) is less than the macshell and Kukui shell carbons; nevertheless its electrical resistivity (0.16 Ω·cm) is almost the same. To gain further insight into this matter we carbonized Leucaena charcoal powder (<105 μm) and measured its resistivity. As displayed in Figure 14a the powder evidences a slightly lower resistivity at the highest compressive pressures employed. On the other hand, the density of the packed bed of powder (0.78 g/mL in Figure 14b) is nearly double that of the 20/40 mesh particles. Taken together these findings indicate that the porosity of a carbonized charcoal does not significantly influence the electrical conductivity of the carbon.

For comparison sake, Espinola et al.[37] reported a resistivity of 1.24 Ω-cm for a packed bed of Babacu nut carbon at 19.6 MPa, and 0.272 Ω-cm at 98 MPa. Likewise, they reported a resistivity of 0.92 Ω-cm for Eucalyptus lignin carbon at 19.6 MPa and 0.19 Ω-cm at 98 MPa. Unfortunately, Espinola et al. did not indicate the HTT of their carbons; consequently, this comparison is not very meaningful.

Discussion

The transformation of biomass to charcoal involves the loss of 60% or more of the substrate's mass with the evolution of nearly four moles of gas per mole of "monomer".[38] During this transformation, the pyranose ring framework of the sugar moieties that compose biomass is grossly rearranged to form aromatic structures. Since this transformation does not involve a liquid phase, many bonds are left dangling; giving rise to a carbonaceous solid that is inherently porous at the molecular level and highly reactive. Rosalind Franklin elucidated some aspects of this transformation in her classic XRD study of crystallite growth in graphitizing and non-graphitizing carbons.[30] She found that oxygen-rich substances (e.g. sugar) form non-graphitizing carbons that have relatively low densities and are micro-porous, very hard, and composed of a randomly oriented, cross-linked structure of graphite-like crystallites. The micro-porous structure combined with the random orientation of the crystallites prevents graphitization, even at HTT as high as 3000 °C. Nevertheless, we remark that Franklin employed a 2 h HTT at 1000 °C prior to carbonization at 2160 °C and higher (sugar charcoal) in her work; whereas we observe graphite-like electrical resistivities following carbonization at 950 to 1050 °C for only 10 min. Surprisingly mild conditions impart graphite-like electrical properties to non-graphitizing carbons.

In a classic paper Mrozowski[18] (see also Pinnick[39]) showed that the electrical resistivity of a packed bed of coke particles (subject to HTT of 1200 °C or more) decreased with increasing pressure (to the -0.5 power) and also decreased with increasing particle size (to the -0.25 power). No limit to the conductivity was reached at pressures as high as 100 MPa. The dependence of resistivity on pressure evidenced hysteresis, and changed with increasing time at constant pres-

sure (i.e. "creep"). On the other hand, we observed no creep, little hysteresis and little effect of pressure on resistivity after an initial compaction of the bed. Furthermore, we found that neither the particle size nor the porosity of the bed had a big impact on its electrical resistivity under a compressive pressure of >5 MPa. We believe that some of these differences can be explained by a crushing of the bed at the high pressures employed by Mrozowski. Our equipment would not accommodate such high compressive pressures. Furthermore, such pressures are not needed to obtain a workable anode in a fuel cell, and stability of the packed bed would be a desirable property of an anode employed in a fuel cell.

If we employ the correlation[40] proposed by Cordero et al. for the higher heating value (HHV) of charcoal (i.e. HHV/MJ = 0.3543 %fC + 0.1708 %VM) and assume that the 950 °C charcoals contain only ash and fixed carbon, then the energy content of these carbons is about 35 MJ/kg (see Table 4). This value is somewhat lower than that of crude oil (ca. 44 MJ/kg), but much higher than most coals. {KT: what about LNG and propane??} Table 4 also displays the energy density of these carbons on a volumetric basis. These values range from 15.2 to 28.6 GJ/m^3, and can be compared to the energy density of gasoline (ca. 28 GJ/m^3; KT: please confirm), ethanol (ca. 21 GJ/m^3; KT: please confirm) LNG (KT??) and propane (KT??). Recognizing that these carbon packed beds retain their density after an initial compaction, it is evident that dense carbon packed beds are attractive energy carriers with energy densities comparable to gasoline.

The 950 °C carbonized charcoals tested in this work spanned a large range of carbon contents, ash contents, H/C and O/C ratios, surface areas, particle sizes, and packed bed densities. Nevertheless, their FTIR spectra, XRD spectra, and their electrical resistivities were quite similar. Furthermore, their FTIR spectra and their electrical resistivities were similar to those of graphite particles. On the other hand, their XRD spectra showed no hint of graphitization at in-

creasing HTT from 750 to 950 °C. These facts cause us to visualize carbonized charcoal to be a macromolecular, cross-linked, amorphous, three dimensional, aromatic structure replete with dangling bonds, nanopores, and micromolecular cracks. If the carbonized charcoal contains graphite crystallites, their scattering domain is less than 3 layers thick. {GV and MT: exactly what evidence have we found for crystallites?? Are there crystallites present at 750 °C?? Please give me your thoughts based on what WE have actually observed, and not what the lore of the field teaches about fossil carbons.}

Conclusions

1. After an initial compaction, a packed bed of carbonized charcoal particles is virtually incompressible and evidences ohmic behavior under a compressive pressure of 7.6 MPa. The contact resistance between the bed and the two electrodes is negligible at this pressure. We observed no creep, little hysteresis, and little effect of pressure on the resistivities of packed beds of carbonized charcoals after the initial compaction.

2. Surprisingly mild conditions (HTT ≈ 950 °C) impart graphite-like electrical properties to all the charcoals that we studied.

3. The electrical resistivity of a packed bed of carbonized charcoal is not strongly dependent upon the particle size of the bed material, the porosity of the bed material, or the apparent density of the packed bed.

4. The energy content of carbonized charcoal (ca. 35 MJ/kg) is somewhat lower than crude oil, but higher than most coals. The energy density of a compact bed of carbonized charcoal (15.2 to 28.6 GJ/m^3) can equal that of gasoline and can exceed that of ethanol. {MJA: more??}

5. Some carbonized charcoals have surprisingly high BET surface areas (e.g. 437 m^2/g); whereas others have negligible surface area. The presence of extremely narrow pores in carbonized charcoals complicates the determination of their surface areas and pore volume distributions.

6. Heat treatment temperatures between 750 and 950 °C have no significant effect on the XRD spectra of macshell charcoals. A wide range of charcoals carbonized at 950 °C manifest nearly identical XRD spectra. The scattering domains in these carbons consist of less than 3 layers.

7. All biocarbons obtained from high-yield macadamia nut shell, leucaena, coconut husk and kukui nut shell charcoals with HTT of 950 °C show very similar FTIR spectra to each other, as well as to the spectrum of graphite.

8. A comparison of the 950 °C biocarbons reveals a considerable range in the values of their C, H, O, and ash contents, and the H/C and O/C ratios. None of these values is closely associated with the electrical conductivity of the biocarbon.

9. The transformation of biomass into a biocarbon semi-metal involves the loss of 60% or more of the substrate's mass with the evolution of nearly four moles of gas per mole of "monomer" of biomass. During this transformation, the pyranose ring framework of the sugar moieties that compose biomass is grossly rearranged to form aromatic structures. Since this transformation does not involve a liquid phase, many bonds are left dangling; giving rise to a carbonaceous solid that is inherently porous at the molecular level and highly reactive. The findings of this work cause us to visualize carbonized charcoal to be a macromolecular, cross-linked, amorphous, three dimensional, aromatic structure replete with conjuagation and dangling bonds,

nanopores, and micromolecular cracks. If the carbonized charcoal contains graphite crystallites, their scattering domain is less than 3 layers thick. {MJA: rewrite this conclusion.}

10. In light of the facts that: (a) a compact packed bed of carbonized charcoal can have an electrical resistivity comparable to that of graphite, and (b) a compact carbonized charcoal packed bed can have a very large surface area and high reactivity as well as an energy density comparable to gasoline, and (c) biomass charcoal has a wholesale price ($6 per GJ) that is comparable to gasoline and natural gas; in the very near future we anticipate the development of batteries and fuel cells that efficiently and economically generate electric power via the electrochemical oxidation of compact packed beds of carbonized charcoal.

Acknowledgments

We thank Lloyd Paredes, Brent Shimizu, Caera McNally, Carolyn Wallace, and Kurt Verheyden (all of UH) for assistance with the experimental work, Prof. Jim Brewbaker (UH) and Dana Gray (Oils of Aloha) for biomass samples, and John Wayte for his skillful fabrication of the apparatus displayed in Figure 1. Research at the University of Hawaii (UH) was supported by the Office of Naval Research (contract #N00014-01-1-0928), the Coral Industries Endowment of UH, and the Osaka Gas Co. Research at the Hungarian Academy of Sciences was supported by OTKA grant T 037705.

List of Table Captions

Table 1. Carbonized charcoals employed in this work.

Table 2. H/C, O/C ratios.

Table 3. Results of the XRD analyses.

Table 4. Summary of the resistivity and density values of packed beds of carbonized charcoal under a compressive pressure of ca. 7.6 MPa.

List of Figure Captions

Figure 1. Apparatus employed to measure the electrical resistivity of a packed bed of carbonized charcoal.

Figure 2. Effect of compressive pressure on the zero offset of the measured bed height. Zero offset values calculated by Hook's law (--). Measured zero offset values (●).

Figure 3. Effect of heat treatment temperature on the FTIR spectra of macadamia nutshell char. The spectrum of the synthetic graphic is shown for comparison. (Each curve is drawn one unit higher than the curve beneath it.)

Figure 4. FTIR spectra of carbons treated at 950°C. (Each curve is drawn one unit higher than the curve beneath it.)

Figure 5. XRD spectra of a natural (—) and a synthetic (- - -) graphite, used as references.

Figure 6. Effect of the heat treatment temperature on the XRD spectra of the macadamia nutshell carbon.

Figure 7. Comparison of the XRD spectra of charcoals carbonized at 950°C.

Figure 8. Resistivity (lower set of curves) and bed length (upper set of curves) vs. compressive pressure for a packed bed of (a) 0.5 g, (b) 1.0 g, (c) 1.5 g of 20/40 mesh AC; (d) ohmic behavior of the carbon packed bed at 7.6 MPa; and (e) resistivity and bed length vs. compressive pressure for a 0.5 g packed bed of <105 μm AC powder. Symbols for (a), (b), (c) and (e) ●: pressurization #1, ○: depressurization #1, ■: pressurization #2, □: depressurization #2. Symbols for (d) ●,■ and solid line: measured resistance for pressurization #1 and #2

and least squares regression line, ⊙,⊡ and dotted line: corrected resistance by subtraction of the empty cell resistance for pressurization #1 and #2 and least squares regression line.

Figure 9. Resistivity (lower set of curves) and bed length (upper set of curves) vs. compressive pressure for a 2.0 g packed bed of 1-2 μm graphite powder. (●: pressurization #1, ○: de-pressurization #1, ■: pressurization #2, □: depressurization #2.)

Figure 10. Resistivity (lower set of curves) and bed length (upper set of curves) vs. compressive pressure for a 1.0 g packed bed of 20/40 mesh carbonized AC. (●: pressurization #1, ○: de-pressurization #1, ■: pressurization #2, □: depressurization #2.)

Figure 11. Resistivity (lower set of curves) and bed length (upper set of curves) vs. compressive pressure for a 0.49 g packed bed of coconut husk carbonized charcoal powder. (●: pressuri-zation #1, ○: depressurization #1, ■: pressurization #2, □: depressurization #2.)

Figure 12. Resistivity vs. compressive pressure for ca. 0.5 g packed beds of 20/40 mesh maca-damia nut shell charcoals carbonized at 650, 750, 850, 950, and 1050 °C, and graphite pow-der (for comparison). Symbols (□: 650°C, ▲: 750°C, ■: 850°C, △: 950°C, ▽: 1050°C, ●: graphite). Each curve shows depressurization #2.

Figure 13. Resistivity (lower set of curves) and bed length (upper set of curves) vs. compressive pressure for a 0.5 g packed bed of 20/40 mesh Kukui shell carbonized charcoal. (●: pres-surization #1, ○: depressurization #1, ■: pressurization #2, □: depressurization #2.)

Figure 14. (a) Resistivity vs. compressive pressure and (b) resistivity vs. apparent density for packed beds of 20/40 mesh and <105 μm Leucaena wood carbonized charcoal. (a) Solid line: 20/40 mesh. Dashed line: powder. Each curve shows depressurization #2. (b) Left side: 20/40 mesh. Right side: powder. (●: pressurization #1, ○: depressurization #1, ■: pressuri-zation #2, □: depressurization #2.)

References cited

(1) Vielstich, W. *Fuel Cells.*; Wiley-Interscience: London, 1965.

(2) Williams, K. R., Ed., *An Introduction to Fuel Cells.*, Elsevier Publishing Co.: Amsterdam, 1966.

(3) Bockris, J. O. M.; Srinivasan, S. *Fuel Cells: Their Electrochemistry.*; McGraw-Hill Book Co.: New York, 1969.

(4) Anbar, M.; McMillen, D. F.; Weaver, R. D.; Jorgensen, P. J. Method and Apparatus for Electrochemical Generation of Power from Carbonaceous Fuels. U.S.A. Patent 3,970,474, 1976.

(5) Anbar, M. Methods and Apparatus for the Pollution-Free Generation of Electrochemical Energy. USA Patent 3,741,809, 1973.

(6) Pesavento, P., personal communication, 1998.

(7) Gur, T. M.; Huggins, R. A. Direct Electrochemical Conversion of Carbon to Electrical Energy in a High Temperature Fuel Cell. *J. Electrochem. Soc.* **1992**, *139*, L95.

(8) Ford, A. R.; Greenhalgh, E. Industrial Applications of Carbon and Graphite. In *Modern Aspects of Graphite Technology*; L. C. F. Blackman, Eds.; Academic Press: London, 1970; p 258.

(9) Coutinho, A. R.; Luengo, C. A. Preparing and Characterizing Electrode Grade Carbons from Eucalyptus Pyrolysis Products. In *Advances in Thermochemical Biomass Conversion*; A. V. Bridgwater, Eds.; Blackie Academic & Professional: London, 1993; p 1230.

(10) Coutinho, A. R.; Luengo, C. A. Mass Balance of Biocarbon Electrodes Obtained by Experimental Bench Production. In *Developments in Thermochemical Biomass Conversion*;

A. V. Bridgwater and D. G. B. Boocock, Eds.; Blackie Academic & Professional: London, 1997; p 305.

(11) Coutinho, A. R.; Rocha, J. D.; Luengo, C. A. Preparing and characterizing bio-carbon electrodes. *Fuel Processing Technology* **2000**, *67*, 93.

(12) Antal, M. J.; Allen, S. G.; Dai, X.; Shimizu, B.; Tam, M. S.; Gronli, M. G. Attainment of the theoretical yield of carbon from biomass. *Ind. Eng. Chem. Res.* **2000**, *39*, 4024.

(13) Antal, M. J.; Dai, X.; Shimizu, B.; Tam, M. S.; Gronli, M. G. New Prospects for Biocarbons. In *Progress in Thermochemical Biomass Conversion*; A. V. Bridgwater, Eds.; Blackwell Science: Oxford, 2001; p 1179.

(14) Dai, X.; Antal, M. J., Jr. Synthesis of a High-Yield Activated Carbon by Air Gasification of Macadamia Nut Shell Charcoal. *Ind. Eng. Chem. Res.* **1999**, *38*, 3386.

(15) Tam, M. S.; Antal, M. J., Jr. Preparation of Activated Carbons from Macadamia Nut Shell and Coconut Shell by Air Activation. *Ind. Eng. Chem. Res.* **1999**, *38*, 4268.

(16) Conesa, J. A.; Sakurai, M.; Antal, M. J. Synthesis of a High-Yield Activated Carbon by Oxygen Gasification of Macadamia Nut Shell Charcoal in Hot, Liquid Water. *Carbon* **2000**, *38*, 839.

(17) Tam, M. S.; Antal, M. J.; Jakab, E.; Varhegyi, G. Activated Carbon from Macadamia Nut Shell by Air Oxidation in Boiling Water. *Ind. Eng. Chem. Res.* **2001**, *40*, 578.

(18) Mrozowski, S. In *Proceedings of the Third Conference on Carbon*; Eds.; Pergamon Press: New York, 1959; p 495.

(19) Varhegyi, G.; Szabo, P.; Till, F.; Zelei, B.; Antal, M. J.; Dai, X. TG, TG-MS, and FTIR Characterization of High-Yield Biomass Charcoals. *Energy Fuels* **1998**, *12*, 969.

(20) Varhegyi, G.; Szabo, P.; Antal, M. J. Kinetics of Charcoal Devolatilization. *Energy Fuels* **2002**, *16*, 724.

(21) Friel, J. J.; Mehta, S.; Follweiler, D. M. Electron Optical and IR Spectroscopic Investigation of Coal Carbonization. In *Coal and Coal Products: Analytical Characterization Techniques.*; E. L. Fuller, Eds.; American Chenmical Society: Washington, DC, 1982; p 294.

(22) Mapelli, C.; Castiglioni, C.; Meroni, E.; Zerbi, G. Graphite and Graphitic Compounds: Vibrational Spectra from Oligomers to Real Materials. *J. Mol. Struct.* **1999**, *480-481*, 615.

(23) Kwizera, P.; Dresselhaus, M. S.; Dresselhaus, G. Raman Spectra and Staging of Intercalated Graphite Fibers. *Carbon* **1983**, *21*, 121.

(24) Kim, D.-Y.; Nishiyama, Y.; Wada, M.; Kuga, S. Graphitization of Highly Crystalline Cellulose. *Carbon* **2001**, *39*, 1051.

(25) Lu, L.; Sahajwalla, V.; Harris, D. Characteristics of Chars Prepared from Various Pulverized Coals at Different Temperatures Using Drop-Tube Furnace. *Energy Fuels* **2000**, *14*, 869.

(26) Yen, T. F.; Erdman, J. G.; Pollack, S. S. *Anal. Chem.* **1961**, *33*, 1587.

(27) Walker, P. L.; Seeley, S. B. Fine Grinding of Ceylon Natural Graphite. In *Proceedings of the Third Conference on Carbon*; Eds.; Pergamon Press: 1959; p 481.

(28) Senneca, O.; Salatino, P.; Masi, S. Microstructural changes and loss of gasification reactivity of chars upon heat treatment. *Fuel Processing Technology* **1998**, *77*, 1483.

(29) Dai, X. *Pyrolytic and Oxidative Syntheses of High-Yield Carbons from Biomass.* Ph.D. Thesis, University of Hawaii at Manoa, Honolulu, HI, 1998.

(30) Franklin, R. Crystallite growth in graphitizing and non-graphitizing carbons. *Proc. Roy. Soc. A* **1951**, *209*, 196.

(31) Marchand, A. *Physico-chemical and structural characterisation of carbons*; Applied Sciences: 1985.

(32) Mantell, C. L. *Carbon and Graphite Handbook*; Interscience: New York, 1968.

(33) McEnaney, B.; Mays, T. J. Porosity in Carbons and Graphites. In *Introduction to Carbon Science*; H. Marsh, Eds.; p 154.

(34) Alekhina, M. B.; Shumyatakii, Y. I.; Skubak, E. A.; Savchenko, S. G. Correlation Between Electrophysical Properties and Parameters of Porous Structure of SKT Activated Charcoal. *Russian J. Applied Chemistry* **1993**, *66*, 1413.

(35) Hutcheon, J. M. Manufacturing Technology of Baked and Graphitized Carbon Bodies. In *Modern Aspects of Graphite Technology*; L. C. F. Blackman, Eds.; Academic Press: London, 1970; p 49.

(36) Golden, T. C.; Jenkins, R. G.; Y. Otake; Scaroni, A. W. Oxygen Complexes on Carbon Surfaces. In *Proceedings of the Workshop on the Electrochemistry of Carbon*; S. Sarangapani, J. R. Akridge, and B. Schumm, Eds.; The Electrochemical Society: Pennington, NJ, 1983; p 61.

(37) Espinola, A.; Miguel, P. M.; Salles, M. R.; Pinto, A. R. Electrical Properties of Carbons-Resistance of Powder Materials. *Carbon* **1986**, *24*, 337.

(38) Antal, M. J.; Gronli, M. G. The Art, Science, and Technology of Charcoal Production. *Ind. Eng. Chem. Res.* **2003**, *in press*,

(39) Pinnick, H. T. *Electronic Properties of Carbons and Graphite*;

(40) Cordero, T.; Marquez, F.; Rodriguez-Mirasol, J.; Rodriguez, J. J. Predicting heating values of lignocellulosics and carbonaceous materials from proximate analysis. *Fuel* **2001**, *80*, 1567.

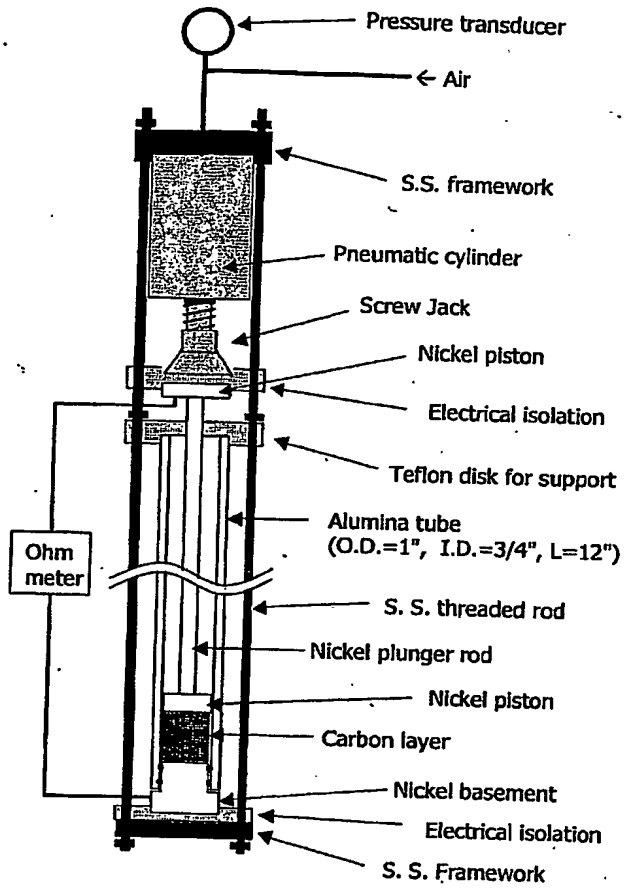

Figure 1. Apparatus employed to measure the electrical resistivity of a packed bed of carbonized charcoal.

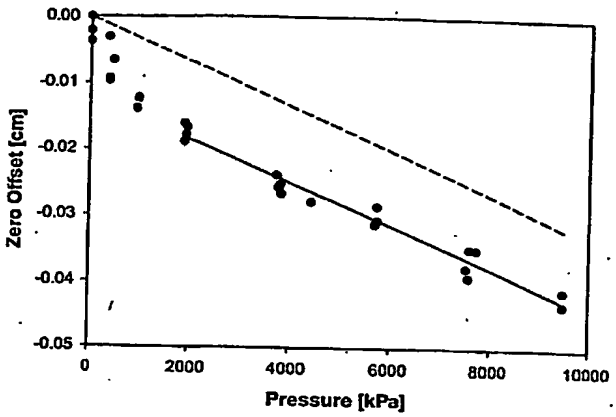

Figure 2. Effect of compressive pressure on the zero offset of the measured bed height. Zero offset values calculated by Hook's law (--). Measured zero offset values (●).

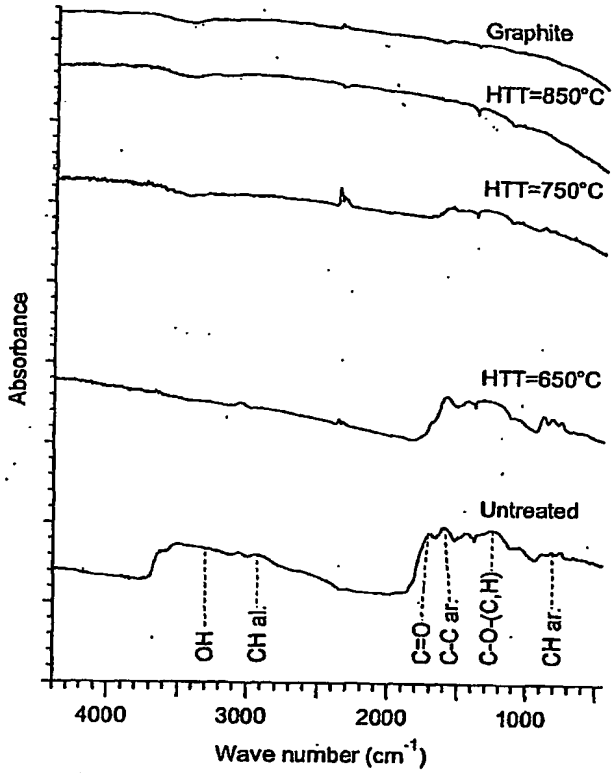

Figure 3. Effect of heat treatment temperature on the FTIR spectra of macadamia nutshell char. The spectrum of the synthetic graphic is shown for comparison. (Each curve is drawn one unit higher than the curve beneath it.)

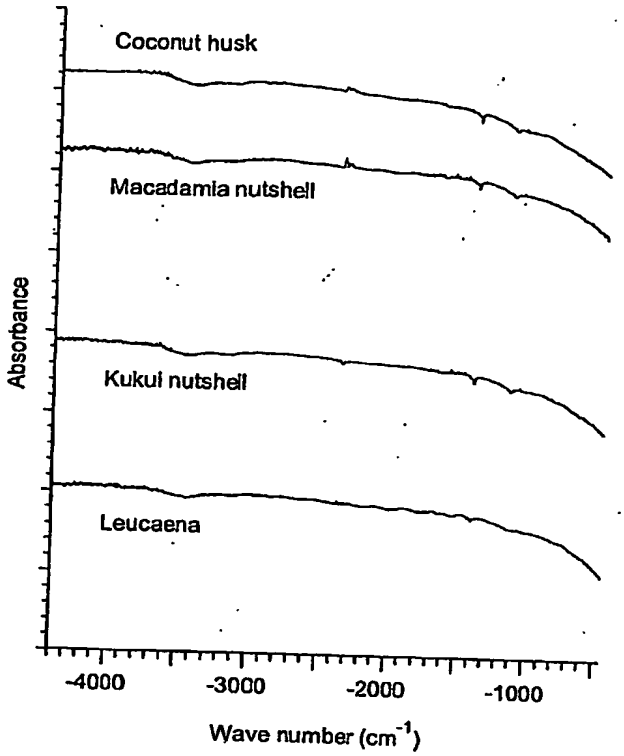

Figure 4. FTIR spectra of carbons treated at 950°C. (Each curve is drawn one unit higher than the curve beneath it.)

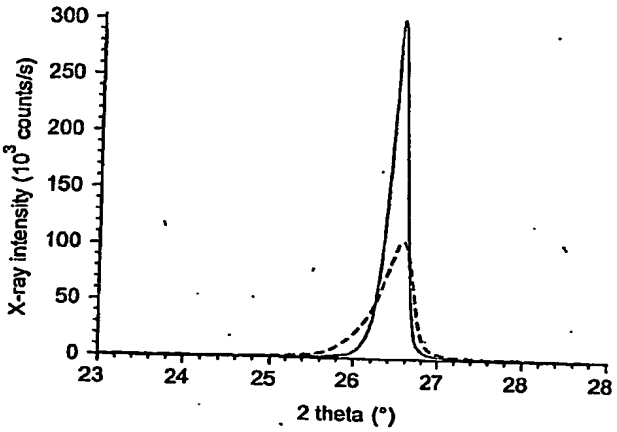

Figure 5. XRD spectra of a natural (—) and a synthetic (- - -) graphite, used as references.

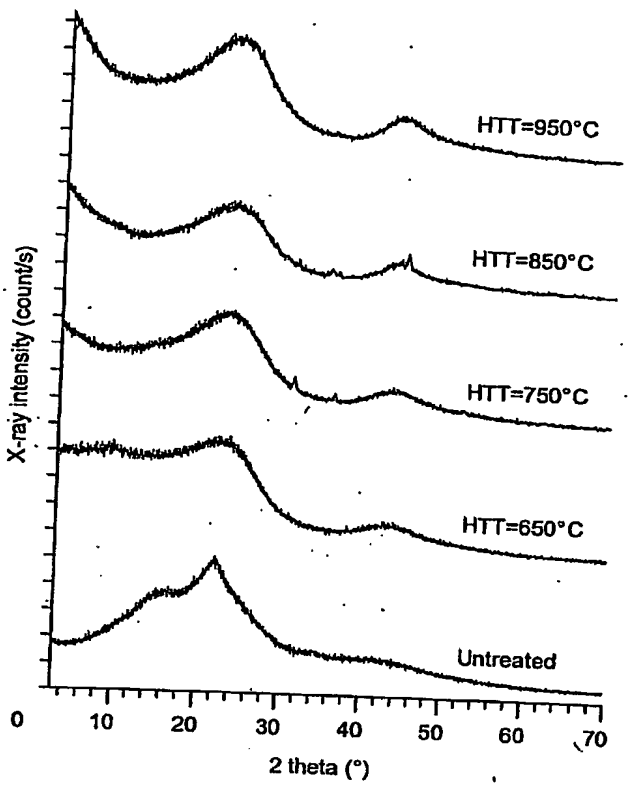

Figure 6. Effect of the heat treatment temperature on the XRD spectra of the macadamia nutshell carbon.

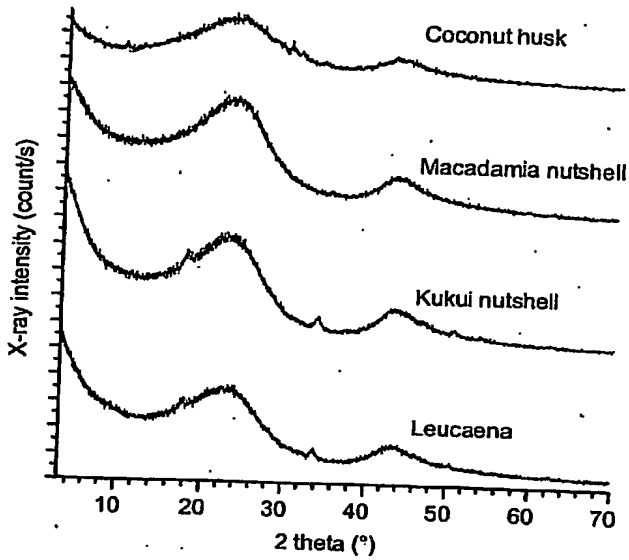

Figure 7. Comparison of the XRD spectra of charcoals carbonized at 950°C.

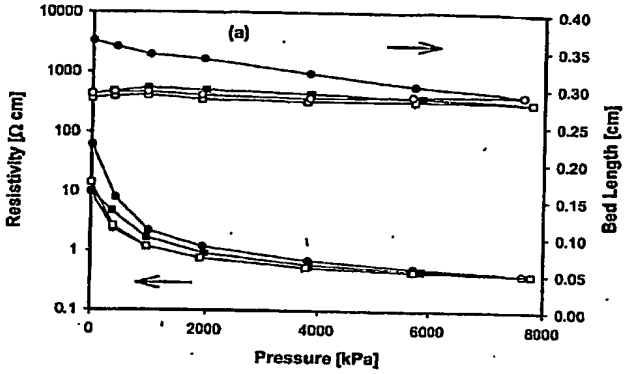
(a)
Resistivity [Ω cm]
Bed Length [cm]
Pressure [kPa]
10000
1000
100
10
1
0.1
0.40
0.35
0.30
0.25
0.20
0.15
0.10
0.05
0.00
0
2000
4000
6000
8000

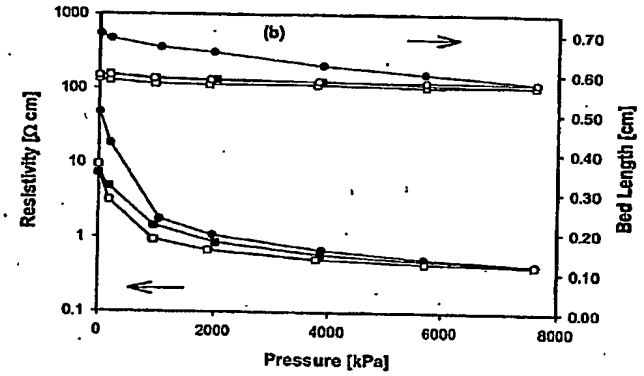
(b)
Resistivity [Ω cm]
Bed Length [cm]
Pressure [kPa]
1000
100
10
1
0.1
0.70
0.60
0.50
0.40
0.30
0.20
0.10
0.00
0
2000
4000
6000
8000

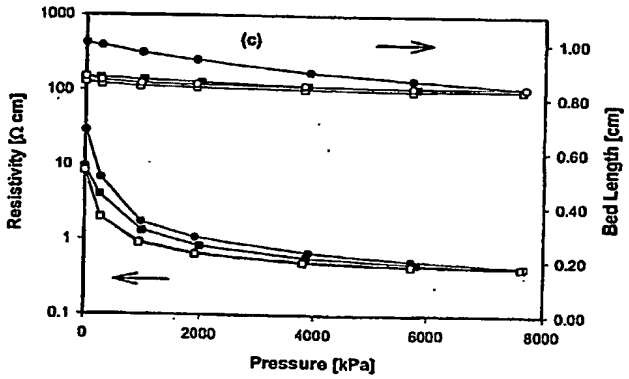
(c)
Resistivity [Ω cm]
Bed Length [cm]
Pressure [kPa]
1000
100
10
1
0.1
1.00
0.80
0.60
0.40
0.20
0.00
0
2000
4000
6000
8000

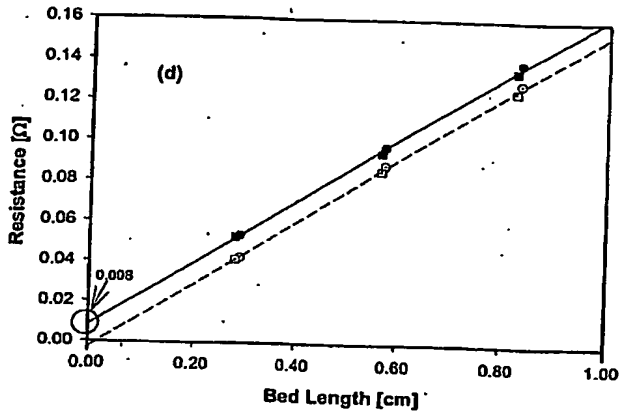

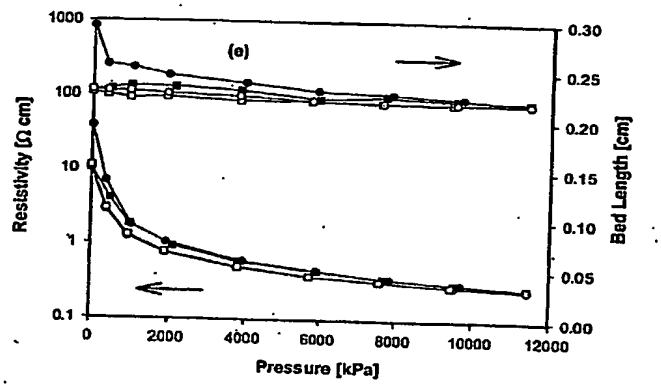

Figure 8. Resistivity (lower set of curves) and bed length (upper set of curves) vs. compressive pressure for a packed bed of (a) 0.5 g, (b) 1.0 g, (c) 1.5 g of 20/40 mesh AC; (d) ohmic behavior of the carbon packed bed at 7.6 MPa; and (e) resistivity and bed length vs. compressive pressure for a 0.5 g packed bed of <105 μm AC powder. Symbols for (a), (b), (c) and (e) ●: pressurization #1, ○: depressurization #1, ■: pressurization #2, □: depressurization #2. Symbols for (d) ●,■ and solid line: measured resistance for pressurization #1 and #2 and least squares regression line, ⊙,⊡ and dotted line: corrected resistance by subtraction of the empty cell resistance for pressurization #1 and #2 and least squares regression line.

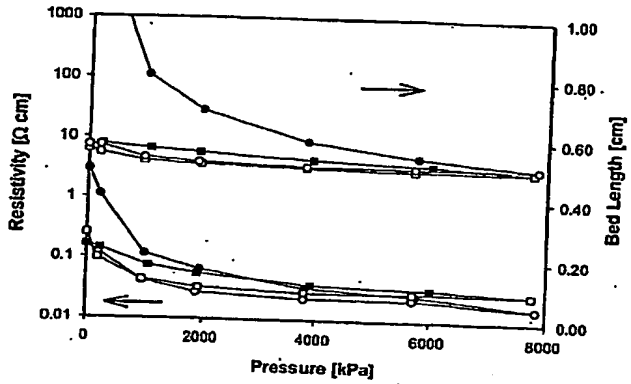

Figure 9. Resistivity (lower set of curves) and bed length (upper set of curves) vs. compressive pressure for a 2.0 g packed bed of 1-2 μm graphite powder. (●: pressurization #1, ○: depressurization #1, ■: pressurization #2, □: depressurization #2.)

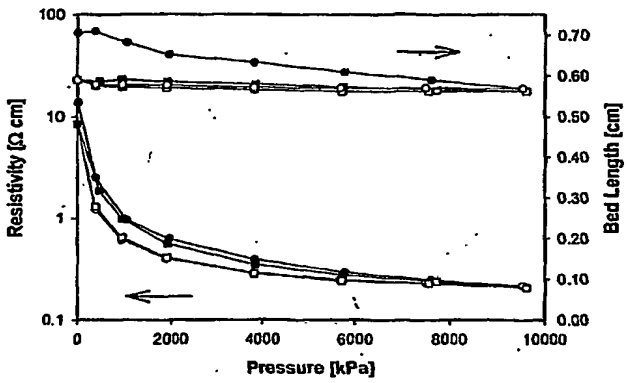

Figure 10. Resistivity (lower set of curves) and bed length (upper set of curves) vs. compressive pressure for a 1.0 g packed bed of 20/40 mesh carbonized AC. (●: pressurization #1, ○: depressurization #1, ■: pressurization #2, □: depressurization #2.)

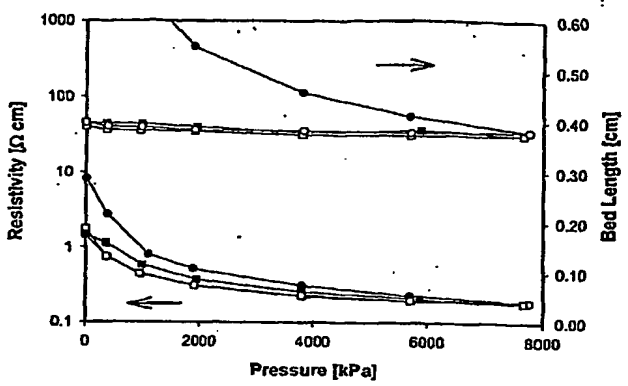

Figure 11. Resistivity (lower set of curves) and bed length (upper set of curves) vs. compressive pressure for a 0.49 g packed bed of coconut husk carbonized charcoal powder. (●: pressurization #1, ○: depressurization #1, ■: pressurization #2, □: depressurization #2.)

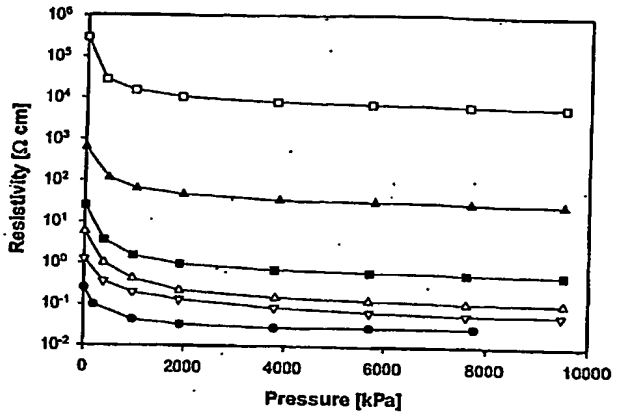

Figure 12. Resistivity vs. compressive pressure for ca. 0.5 g packed beds of 20/40 mesh macadamia nut shell charcoals carbonized at 650, 750, 850, 950, and 1050 °C, and graphite powder (for comparison). Symbols (□: 650°C; ▲: 750°C, ■: 850°C, △: 950°C, ▽: 1050°C, ●: graphite). Each curve shows depressurization #2.

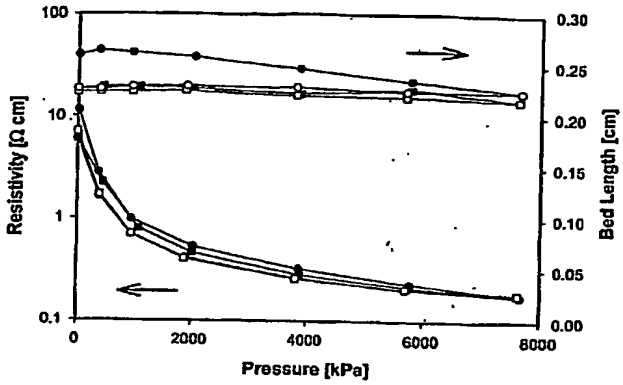

Figure 13. Resistivity (lower set of curves) and bed length (upper set of curves) vs. compressive pressure for a 0.5 g packed bed of 20/40 mesh Kukui shell carbonized charcoal. (●: pressurization #1, ○: depressurization #1, ■: pressurization #2, □: depressurization #2.)

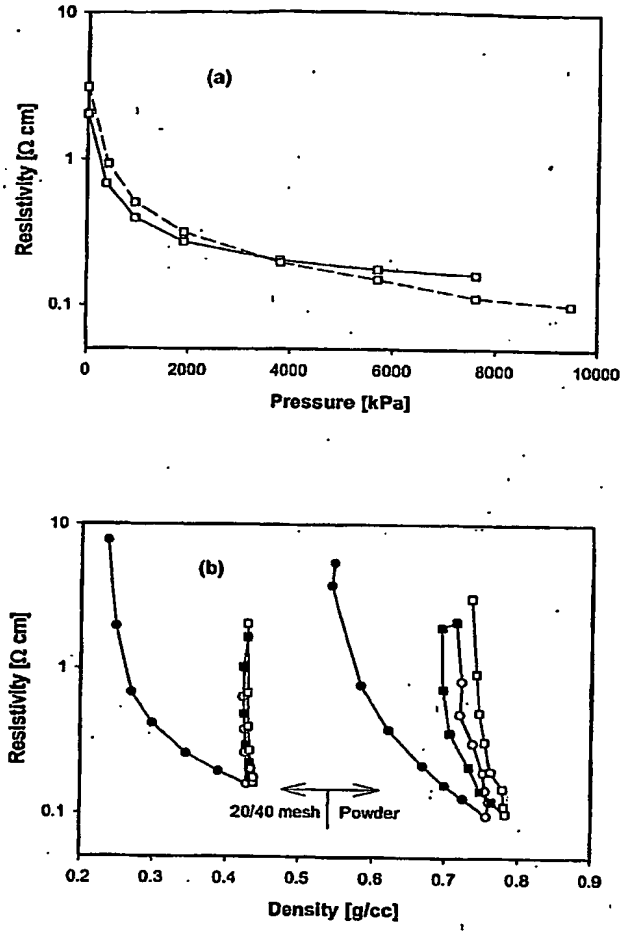

Figure 14. (a) Resistivity vs. compressive pressure and (b) resistivity vs. apparent density for packed beds of 20/40 mesh and <105 μm Leucaena wood carbonized charcoal. (a) Solid line: 20/40 mesh. Dashed line: powder. Each curve shows depressurization #2. (b) Left side: 20/40 mesh. Right side: powder. (●: pressurization #1, ○: depressurization #1, ■: pressurization #2, □: depressurization #2.)

Table 1. Carbonized Charcoals Employed in This Work

Feed	HTT[c] °C	Burnoff[f] wt%	Surface area[g] m^2/g	Pore volume mL/g	Elemental Analyses[h] C	H	O	N	S	Ash
Macnut shell[a]	650	21	216	0.135	87.90%	2.19%	6.69%	1.04%	0.05%	1.17%
	750	22	169	0.115	90.71%	1.63%	5.97%	0.95%	0.05%	1.12%
	850	30	194	0.132	90.03%	0.89%	5.66%	1.00%	0.06%	4.51%
	950	32	244	0.164	89.98%	0.90%	6.04%	1.11%	0.05%	1.61%
	1050	22	NA	NA	95.13%	0.37%	2.82%	1.43%	0.05%	1.07%
Kukui nut shell[b]	950	NA[i]	22	NA	92.92%	0.54%	4.52%	1.26%	<0.05%	1.49%
Coconut husk[c]	950	NA	437	NA	85.08%	0.72%	8.39%	0.91%	0.05%	5.63%
Leucaena wood[d]	950	NA	310	NA	92.15%	0.46%	3.99%	1.15%	0.05%	2.45%

[a] High-yield charcoal 961205 except 1050 °C, that was flash-carbonization charcoal 020510. [b] High-yield charcoal 941114. [c] High-yield charcoal 941202. [d] High-yield charcoal 940721. [f] Weight loss during carbonization. [g] BET surface area. [h] Performed by the Huffman Lab. Values in wt%. [i] NA = not available.

Table 2. H/C and O/C Ratios[a] for the Carbonized Charcoals Employed in This Work

Feed	HTT °C	H/C	O/C
Macadamia nut shell	650	0.2969	0.0571
	750	0.2141	0.0494
	850	0.1178	0.0472
	950	0.1192	0.0504
	1050	0.0463	0.0223
Kukui nut shell	950	0.0693	0.0365
Coconut husk	950	0.1008	0.0740
Leucaena wood	950	0.0595	0.0325

[a] Ratios on a mole basis.

Table 3. Results of the XRD Analyses. {GV: please make this Table like the others. Some small adjustments are needed.}

Feed	HTT	FWHM[a]	L_{002}[b]	ε[c]	d (002)[d]	γ_a[e]
	°C	(°2Θ)		%		
Macnut shell	-	8.69	6	19.18	4.01	0.74
	650	8.44	7	17.91	3.98	0.79
	750	7.98	7	16.81	3.87	0.96
	850	7.78	8	16.25	3.79	0.97
	950	7.77	8	16.27	3.76	0.99
Kukui nut shell	950	8.01	7	16.91	3.85	0.99
Coconut husk	950	9.67	6	22.76	3.89	0.99
Leucaena wood	950	8.66	6	18.72	3.83	0.99
Synth. graphite		0.45	233	0.81	3.35	0.997
Natural graphite		0.18	918	0.29	3.36	0.995

[a] FWHM: Width at half peak height of reflection (002)

[b] L_{002}: Domain size calculated by Fourier and Voigt analysis, using the Scherrer equation

[c] ε: Deformation

[d] d (002): Distance between crystallite planes in direction (002)

[e] γ_a: aromaticity factor

Table 3 Summary of the resistivity and density values of packed beds of carbon under a compressive pressure of ca. 7.6MPa

Feed	HTT °C	Particle Size[b] -	Sample Weight g	Resistivity[c] Ω cm	Density[c] g/cc	Energy Content[d] MJ/kg	Energy Density[d] GJ/m^3
Macadamia nut shell	650	20/40	0.24	$6.6*10^{3}$	0.70	35.0	24.5
	750	20/40	0.37	$2.9*10^{1}$	0.65	35.0	22.8
	850	20/40	0.45	$5.8*10^{-1}$	0.65	33.8	22.0
	950	20/40	0.50	$1.1*10^{-1}$	0.58	34.9	20.2
	1050	20/40	0.51	$5.9*10^{-2}$	0.61	35.1	21.4
Kukui nut shell	950	20/40	0.50	$1.8*10^{-1}$	0.82	34.9	28.6
Coconut husk	950	20/40	0.49	$1.8*10^{-1}$	0.46	33.4	15.4
Leucaena wood	950	20/40	0.50	$1.6*10^{-1}$	0.44	34.6	15.2
	950	<105µm	0.50	$1.1*10^{-1}$	0.78	34.6	27.0
Activated carbon	-	20/40	0.51	$4.2*10^{-1}$	0.63	NA	NA
	-	20/40	1.00	$4.3*10^{-1}$	0.62	NA	NA
	-	20/40	1.50	$4.3*10^{-1}$	0.64	NA	NA
	-	<105µm	0.50	$3.3*10^{-1}$	0.81	NA	NA
Carbonized AC[a]	950	20/40	1.00	$2.3*10^{-1}$	0.63	NA	NA
Synthetic graphite	-	1-2 µm	2.00	$2.9*10^{-2}$	1.41	NA	NA

[a] AC = activated carbon. This sample was carbonized in the muffle furnace with a soak time of 10min. [b] measured as U.S. standard sieve size or particle size before the heat treatment. [c] Resistivity and density values upon the 2nd depressurization. [d] Estimated using the correlation of Cordero et al. (see text).

BEST AVAILABLE IMAGES

Defective images within this document are accurate representations of the original documents submitted by the applicant.

Defects in the images include but are not limited to the items checked:

- [x] BLACK BORDERS
- [x] IMAGE CUT OFF AT TOP, BOTTOM OR SIDES
- [x] FADED TEXT OR DRAWING
- [ ] BLURED OR ILLEGIBLE TEXT OR DRAWING
- [ ] SKEWED/SLANTED IMAGES
- [x] COLORED OR BLACK AND WHITE PHOTOGRAPHS
- [ ] GRAY SCALE DOCUMENTS
- [ ] LINES OR MARKS ON ORIGINAL DOCUMENT
- [ ] REPERENCE(S) OR EXHIBIT(S) SUBMITTED ARE POOR QUALITY
- [ ] OTHER: _____

IMAGES ARE BEST AVAILABLE COPY.
As rescanning documents *will not* correct images problems checked, please do not report the problems to the IFW Image Problem Mailbox